2020 17th International Conference on Electrical Engineering, Computing Science and Automatic Control (CCE)
Mexico City, Mexico. November 11-13, 2020

Photoluminescence emission under thermal annealing of Silica and Titania nanospheres arrays

Carina Gutierrez
Optics
National Institute for Astrophysics Optics and Electronics.
Puebla, Mexico.
carina.gutierrez@inaoep.mx

Mario Moreno
Electronics
National Institute for Astrophysics Optics and Electronics.
Puebla, Mexico.
mmoreno@inaoep.mx

Ponciano Rodríguez
Optics
National Institute for Astrophysics Optics and Electronics.
Puebla, Mexico.
ponciano@inaoep.mx

Leticia Tecuapetla
Electronics
National Institute for Astrophysics Optics and Electronics.
Puebla, Mexico.
tecuap@inaoep.mx

Armando Hernandez
Electronics
National Institute for Astrophysics Optics and Electronics.
Puebla, Mexico.
ahdz@hotmail.com

Adrian Itzmoyotl
Faculty of Electronics Science
Meritorious University Autonomous of Puebla
Puebla, Mexico
aitzmo@hotmail.com

***Abstract*— Experimental results on the influence of the annealing time on the photoluminescence (PL) emission of silica array is presented. Bilayers of titania and silica with a thickness of 100 nm and 600 nm, respectively were uniformly deposited on crystalline silicon (c-Si) substrates, and exposed to annealing process from 0 to 60 minutes in intervals of 10 minutes at 1100°C in a nitrogen atmosphere. Our results showed that annealed samples during 30 minutes present PL emission 110 times larger than samples without annealing. Influence of the nanoparticles array distribution on the PL intensity before and after the annealing process is also presented.**

Keywords— Silica, Titania, nanospheres, photoluminescence, layers.

I. INTRODUCTION

Due to its high thermal stability, high chemical durability, low thermal expansion coefficient and adjustable refractive index, titania (TiO_2) and silica (SiO_2) based films have been widely used for several optics applications [1]. Moreover, the photoluminescence (PL) properties of titania and silica nanoparticles (NPs) are employed for multiple research projects and for a large number of optoelectronics and photonic applications [2].

Some optoelectronic circuits are fabricated from materials that do not emit light efficiently, which limits the integration of light sources in the system [3]. To solve this inconvenient, several techniques have been proposed to improve the efficiency of the light source, including thermal annealing.

Photoluminescence (PL) and the mechanism of light emission in thermally annealed thin films have been widely studied, for example, in the silicon excess in silicon-rich oxide (SRO) films and TiO_2-SiO_2 films. Performance of the dependence of the PL peak energy and its intensity enhancement as a function of the annealing time was studied in Refs [4] and [5]. The studied films exhibited a PL band in the 1.4-2.1 eV range after to be exposed at 1100°C for 1, 3 and 5 hours [6]–[8]. The temperature modifies the size and structure of the nanocrystals (nCs); for low temperature (900°C) the nCs presented lower crystallinity compared with samples annealed at higher temperature (1000 and 1100°C) [2]. Increasing the size of nCs leads the PL emission at longer wavelengths (red shift). The light emission is explained according to quantum confinement model. Experimentally, it was found that the nCs average size is not increased when the films were exposed to prolonged thermal annealing.

In semiconductors nanoscience, the ability to control the size and shape (i.e. nanospheres, nanopillars and nanofibres) of colloidal nanomaterials provide more flexibility and options for the design of new materials to different applications [9]. Several structures have been studied after a high temperature annealing; generally, they shown a structural transformation and an increase on the photoluminescence. Our interest is on spherical nanostructures, in particular silica and titania nanospheres. The individual characterization of these NPs are reported in previous works [10], [11]. For instance, the PL emission of silica NPs with Ce and Tb core exposed to a thermal annealing present a dependence with the particle size; after to be annealed at 700°C for 3 hours the NPs with diameter of 600 nm and 1200 nm show a PL intensity of 15000 a.u. and 45000 a.u., respectively [8]. However, there are few studies into luminescence of titania nanoparticles after an annealing

978-1-7281-8987-1/20/$31.00 ©2020 IEEE

process. In ref [12] TiO_2 nanofibres annealed at high temperature have been investigated and characterized. Temperature range from 0 to 1000°C was used to achieve the crystalline phase transformation from anatase to rutile. The PL emission presented dominants bands from 2.56 to 1.32 eV. These results were explained by the change of surface traps levels, which are induced by the presence of oxygen vacancies [9], [11].

Our proposal is to experimentally study the enhancement of light emission of a nanostructure array annealed at high temperatures and short times without the use of core-shell structure or the implantation of additional materials. In this report, we present results on photoluminescence enhancement using nanoparticles array of silica and titania, of diameter de 600 nm and 100 nm, respectively. We choose silica and titania nanoparticles because of its outstanding optical trap properties. Silica-titania array presented has silica NPs as the bottom layer and titania NPs on the top layer.

II. Experimental

A. Materials

Silica (SiO2) nanoparticles (NPs) with average diameter (d1) of 600 nm at 5wt% in water and Titania (TiO2 rutile) high purity NPs with average diameter (d2) of 100 nm diameter at 20wt% in water were purchased from NanoCym and US Research Nanomaterials, Inc., respectively. As substrates we employed [100] crystalline silicon (c-Si) wafers.

B. Substrate preparation

c-Si substrates were prepared using two process. The first process was the cleaning process: the substrates were immersed in an ultrasonic shower with Trichloroethylene (TCE) and then in acetone, 10 min for each solvent, washed three times in deionized water and dried by centrifuge. The second process one makes the surface hydrophilic: the substrates were exposed in oxygen plasma at 300W and 250mTorr for 240s.

C. Colloidal solution preparation

Silica and titania nanoparticles were received as a colloidal suspension in water. The NPs were dispersed in a ratio of 1:3 and 1:2, respectively, with a solution of the surfactant Triton X-10 and methanol at 1:400 by volume [13], [14]. The NPs suspensions were sonicated for 30 min to avoid agglomeration.

D. Nanospheres deposition

Three periodic silica and titania nanoparticles arrays were deposited on c-Si substrates of size 1x1 inches. The first array is a silica NPs monolayer, the second array is a titania NPs monolayer, they were deposited on the substrate by spin coating at 1500 rpm and 4000 rpm [15], respectively; experimentally we found that these spin speeds allows the formation of uniform layers on the substrate and produces a periodic hexagonal closed-packed array, see Figure 1a and b. The third array is a silica-titania NPs bilayer; silica NPs form the bottom monolayer and titania NPs form the top monolayer, the NPs layers were deposited at spin speeds of 1500 rpm and 4000 rpm, respectively, see Figure 1c. Each NPs layer was dried at 80°C for 10 minutes over a hotplate.

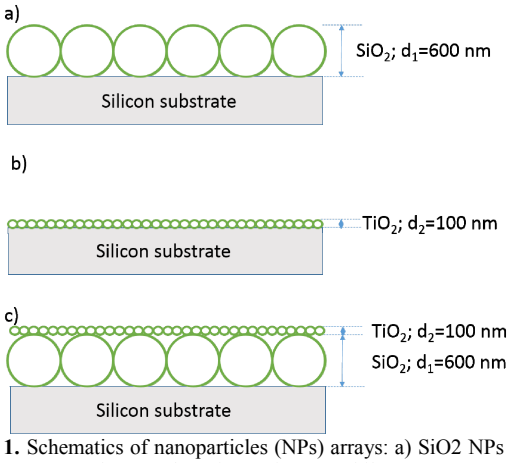

Figure 1. Schematics of nanoparticles (NPs) arrays: a) SiO2 NPs monolayer, b) TiO2 NPs monolayer and c) SiO2 -TiO2 NPs bilayer.

E. Thermal annealing of NPs bilayer array

The silica-titania samples were annealed at 1100°C during 10, 20, 30, 40, 50 and 60 minutes in a tube furnace with a flat quartz holder, under a nitrogen atmosphere at ambient pressure.

F. Characterization equipment

The periodical NPs distribution was visualized by a Scanning Electron Microscope (SEM) Hitachi, model SU3500. Photoluminescence spectra were recorded at room temperature in the wavelength range of 370-1000 nm using a photomultiplier tube as signal detector. The 3.54 eV (350 nm) emission line of a continuous light source xenon arc-lamp was used for the excitation.

III. Results and Discussion

A. Morphology

Figure 2 shows the images of the three arrays before they were annealed. These images were obtained using the Scanning Electron Microscopy. The Figure 2a shows the distribution of the silica NPs monolayer obtained at a spin speed of 1500 rpm, it is a uniform distribution with a visible periodic hexagonal closed-packed array. The Figure 2b shows the titania NPs monolayer, the near spherical NPs morphology does not enable visualize the hexagonal periodic layer, however a uniform distribution is reached at 4000 rpm. The Figure 2c shows the image of the silica-titania NPs bilayer, the top layer of titania NPs present some agglomerations as a result from irregularities of the bottom monolayer of silica

NPs; the layers were deposited at spin speeds of 1500 rpm for the silica and 4000 rpm for the titania.

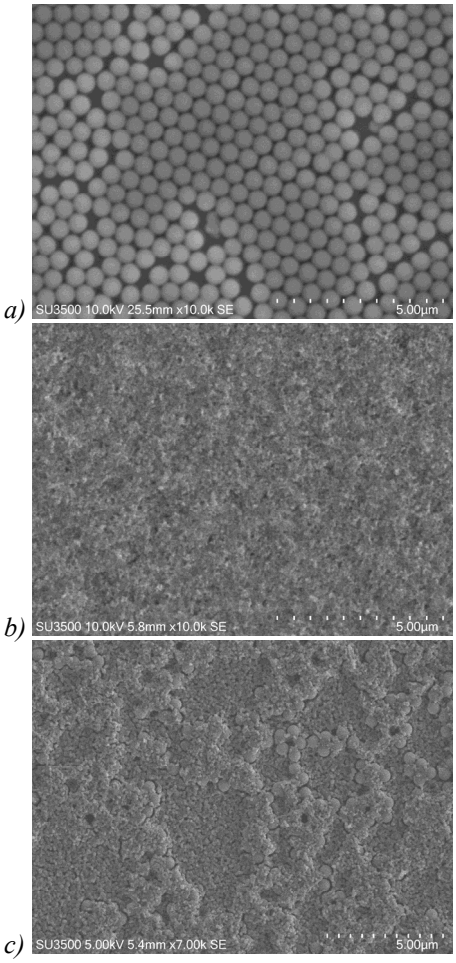

Figure 2. SEM images of silica and titania NPs distribution: a) monolayer of silica NPs with 1:3 concentration deposited at 1500 rpm, b) monolayer of titania NPs with 1:2 concentration deposited at 4000 rpm, c) bilayer: the bottom layer is made with silica NPs with 1:3 concentration deposited at 1500 rpm and the top layer is made with titania NPs with 1:2 concentration deposited at 4000 rpm..

B. Photoluminescence properties

Figure 3 shows the PL spectra of silica NPs and titania NPs monolayers. The black line is the emission spectra of silica NPs; it presents two peaks, the first one has an amplitude about 5000 a.u. in the wavelength range of 400-450 nm, the second one is a broad peak with lower amplitude of about 840 a.u. in the wavelength range of 720-870 nm. The red line is the emission spectra of titania NPs, it presents two broad and small peaks (as compared to the first peak of the silica); the first one has an amplitude about 1000 a.u. in the wavelength range of 460-580 nm, the second peak is about 700 a.u. in the wavelength range of 840-970 nm. These experimental PL amplitudes and wavelength range are consistent with reported values in the literature [2], [9].

Figure 4a shows typical PL emission spectra of a silica-titania bilayer sample before thermal annealing ("0 minutes"). It presents two relatively broad peaks with low amplitudes; the amplitude of the first peak is about 700 a.u. in the wavelength range 380-450 nm, while the amplitude of the second one is about 500 a.u. in the wavelength range of 700-900 nm. Figure 4b presents the PL emission of annealed silica-titania samples from 10 to 60 minutes in intervals of 10 minutes at 1100°C. It is observed that after thermal annealing the samples present a main emission in the range from 700 to 900 nm and a negligible emission in the range from 400-700 nm. The maximum PL intensity is about 19000 a.u. in the same wavelength range (700-900 nm) for samples annealed during 30 minutes; the amplitude of this peak is 38 times higher than the samples not annealed. For annealing times of 10, 20, 40, 50 and 60 minutes, the amplitudes of the peak emission are about 4500, 4350, 2900, 4500 and 2850 a.u., respectively.

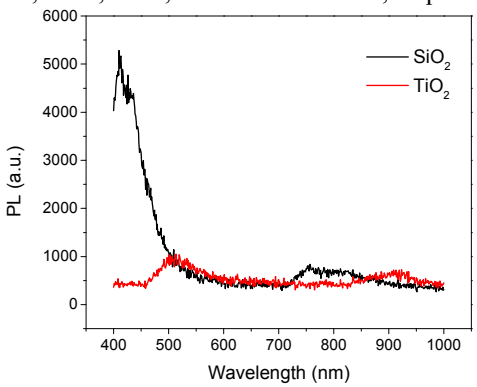

Figure 3. PL spectra of samples coated with a monolayer of: (black line) Silica NPs of 600 nm of diameter with concentration of 1:3 deposited at 1500 rpm, (red line) Titania NPs of 100 nm of diameter with 1:2 concentration deposited at 4000 rpm. The excited wavelength was 350 nm.

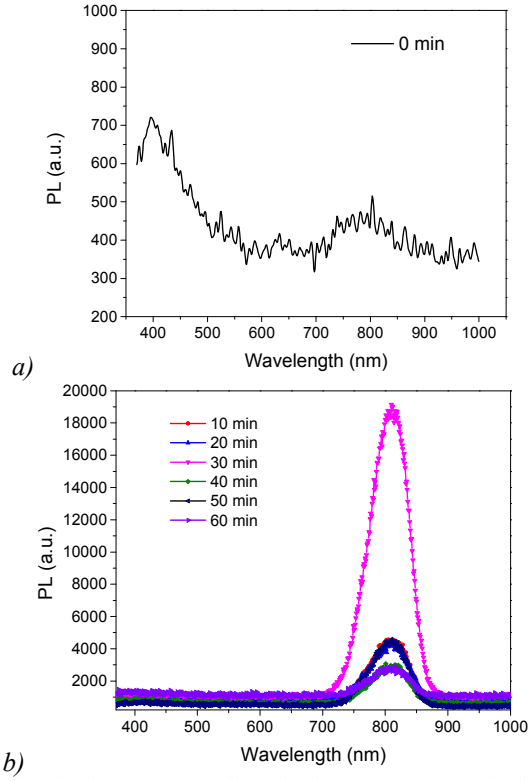

Figure 4. Photoluminescence of silica-titania arrays: a) sample before annealing process, b) samples annealed from 10 to 60 minutes at 1100°C.

In Figure 5, we plot the amplitude of the maximum PL emission of the silica-titania samples as a function of the annealing time from 0 (not annealed) to 60 minutes at 1100°C. This plot shows very clearly the increment of PL emission described before. As stated before, the samples annealed for 30 minutes present the largest photoluminescence emission.

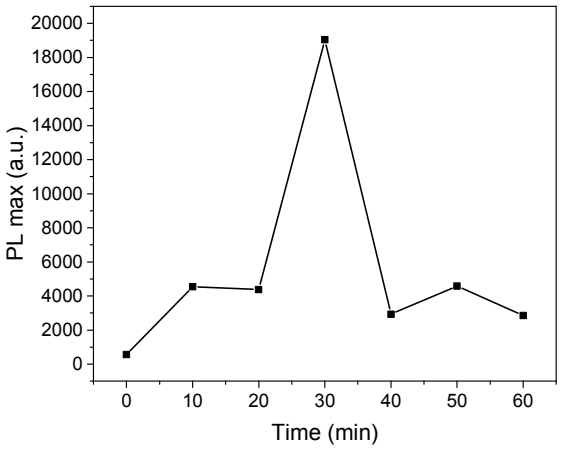

Figure 5. Maximum PL intensity of silica-titania NPs array in function of time annealing.

To understand the mechanism of emission in the silica-titania array, we analyzed the PL spectra by multi-Gaussian deconvolution. Figure 6 depicts the experimental PL spectra of silica-titania array when: a) the sample is no annealed and b)-c) when the samples were annealed at 1100° C for 30 and 60 minutes respectively. We applied a Gaussian fit to the PL spectra. Also, we considered the range of PL peak intensities reported in the literature for the titania and silica nanoparticles when they are exposed to the thermal annealing [2], [4], [6], [9], [10]. The silica NPs emission correspond to the superposition of the Gaussian peaks labeled with numbers (1) and (3); and for the titania NPs emission, the Gaussian peaks are labeled with (2) and (4). According to the fit, the peaks are centered at: (1) 399-407 nm, (2) 395-450 nm, (3) 775-785 nm and (4) 814-882 nm with FWHM of 52-60 nm (3) and 47-52 nm (4).

.

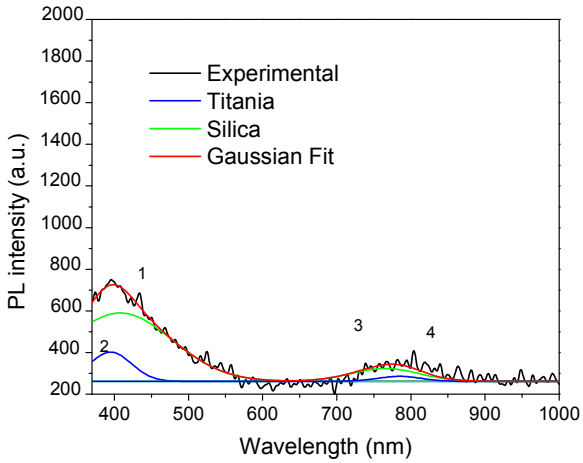

a)

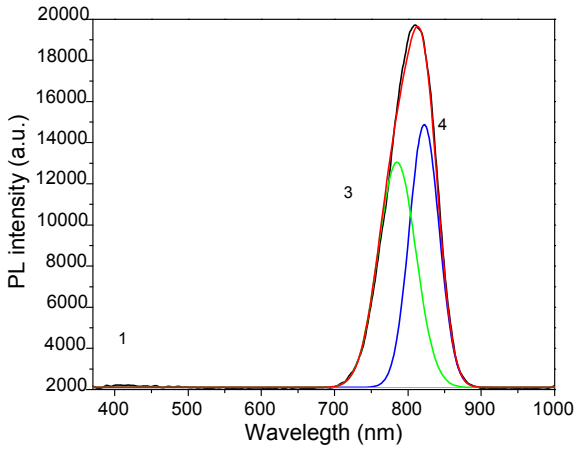

b)

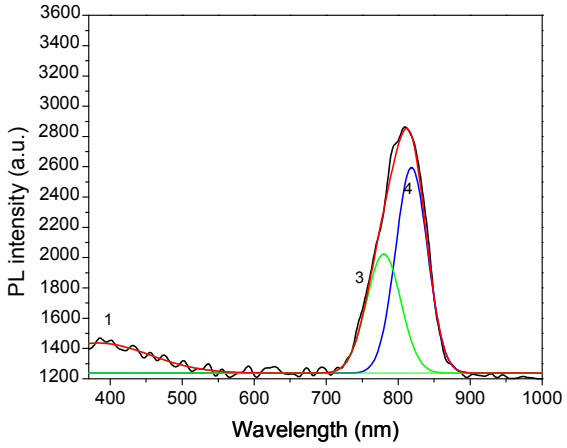

c)

Figure 6. PL spectra and Gaussian fit of the silica-titania NPs array: a) sample without thermal annealing; b) thermally annealed sample at 1100°C for 30 minutes and c) thermally annealed sample at 1100°C for 60 minutes. Black line is the experimental data, green lines are component emission contribution of silica (peaks 1 and 3) and titania (peaks 2 and 4), and red line is the Gaussian fit.

As it is shown in Figures 4 and 6, the emission of the silica and titania bilayer was modified after the thermal annealing. According to the Gaussian fit, for the sample without annealing (Figure 6a), the peaks associated to silica (peaks 1 and 3) are in a range of 410-436 nm and 718-783 nm, respectively; while the peaks associated to titania, the peaks 2 and 4 are in the ranges 424-437 nm and 743-820 nm, respectively. For the sample annealed during 30 minutes (Figure 6b); the maximum emission is for peaks 3 and 4, which are associated to silica and titania, respectively; the peak 3 is in 785 nm and peak 4 is in 822 nm, with amplitudes of 12400 and 14200 a.u., respectively. For the sample annealed during 60 minutes (Figure 6c), the peaks 3 and 4 decreased as compared to the previous sample, the peak 3 is in 779 nm and peak 4 is in 822 nm, with amplitudes of 2000 and 2600 a.u., respectively.

The wavelength ranges and the peak amplitudes suggest that the emission mechanism for titania can be associated with the presence of oxygen vacancies, this is so because while the annealing temperature increases, the oxygen molar

concentration decreases and the titanium concentration increases as well. Also, there is a crystalline phase transformation [9]. For the case of silica, it has been reported theoretically and experimentally that annealing at 1100°C for long time, causes an increase on the number of nanocrystals (nC) with large size, but the average size of the nC remains almost the same, so it is expected a decrease in the number of nC of intermediate size. When the number of smalls nC increases, some of them contributes to the Quantum Confinement of excitons (*Q*) and others to the energy transfer between nanocrystals (*I*). Therefore the whole PL spectra increases as the intensity of both *Q* and *I* increase [2]. Nevertheless, prolongated annealing time can remove nonradiative centers without increasing the nanocrystal size, and therefore PL emission could be associated to the increase of the contribution of *I*.

CONCLUSIONS

Silica-titania nano particles array was deposited by the spin coating technique at room temperature. Bilayers of titania and silica nanoparticles were annealed from 0 to 60 minutes in intervals of 10 minutes at 1100°C in a nitrogen atmosphere. The images of the NPs array, visualized with a SEM; shown a uniform distribution over the c-Si substrates. The photoluminescence of each sample was measured at room temperature, and the maximum photoluminescence (in the range of 700-900 nm) was obtained for the silica-titania arrays samples annealed for 30 minutes; compared with non-annealed samples the later sample shown a 110 fold improvement in the maximum PL intensity. The contribution of each material to the PL spectra was analyzed with a multi-Gaussian deconvolution; analysis of these results suggest that the titania has a larger contribution to the PL intensity at 822 nm, while the silica contribution is lower with a peak at 785 nm.

REFERENCES

[1] P. Yang, D. Xu, D. R. Yuan, C. F. Song, and M. K. Lu, "Structure and photoluminescence properties of sol – gel TiO 2 – SiO 2 films," vol. 413, pp. 155–159, 2002.

[2] E. Tu, "Investigation of Photoluminescence Mechanisms from Regime by Deconvolution of Photoluminescence Spectra," 2016.

[3] S. Y. Lien, D. S. Wuu, W. C. Yeh, and J. C. Liu, "Tri-layer antireflection coatings (SiO2/SiO2-TiO2/TiO2) for silicon solar cells using a sol-gel technique," *Sol. Energy Mater. Sol. Cells*, vol. 90, no. 16, pp. 2710–2719, 2006.

[4] "Silicon-Rich Oxide Obtained by Low-Pressure Chemical Vapor Deposition to Develop Silicon Light Sources," no. Cvd.

[5] J. Barreto and C. Dom, "Optical characterization of silicon rich oxide films," vol. 142, pp. 12–18, 2008.

[6] I. Romanov *et al.*, "Structural Evolution and Photoluminescence of SiO 2 Layers with Sn Nanoclusters Formed by Ion Implantation," vol. 2019, pp. 10–12, 2019.

[7] V. Nikas, S. Gallis, M. Huang, and A. E. Kaloyeros, "Thermal annealing effects on photoluminescence properties of carbon-doped silicon-rich oxide thin films implanted with erbium," *J. Appl. Phys.*, vol. 109, no. 9, 2011.

[8] M. Yu, H. Wang, C. K. Lin, G. Z. Li, and J. Lin, "Sol – gel synthesis and photoluminescence SiO 2 @ LaPO 4 : Ce 3 + / Tb 3 + particles with a," vol. 3245.

[9] I. C. MirjanPhotoluminescence of Anatase and Rutile TiO 2 Particles †a, M. D. Dramic, D. J. Jovanovic, S. P. Ahrenkiel, and J. M. Nedeljkovic, "Photoluminescence of Anatase and Rutile TiO 2 Particles †," pp. 25366–25370, 2006.

[10] "Structural and optical characterization of the crystalline phase transformation of electrospinning TiO 2 nanofibres by high temperatures annealing," vol. 65, no. October, pp. 459–467, 2019.

[11] P. Account, "Atomic Defects in Titanium Dioxide," pp. 923–934, 2014.

[12] H. Nakajima, T. Mori, Q. Shen, and T. Toyoda, "Photoluminescence study of mixtures of anatase and rutile TiO2 nanoparticles: Influence of charge transfer between the nanoparticles on their photoluminescence excitation bands," *Chem. Phys. Lett.*, vol. 409, no. 1–3, pp. 81–84, 2005.

[13] J. C. Hulteen and R. P. Van Duyne, "Nanosphere lithography: A materials general fabrication process for periodic particle array surfaces," *J. Vac. Sci. Technol. A Vacuum, Surfaces, Film.*, vol. 13, no. 3, pp. 1553–1558, 2002.

[14] T. R. Jensen, M. D. Malinsky, C. L. Haynes, and R. P. Van Duyne, "Nanosphere Lithography: Tunable Localized Surface Plasmon Resonance Spectra of Silver Nanoparticles," *J. Phys. Chem. B*, vol. 104, no. 45, pp. 10549–10556, 2002.

[15] S. Das, C. Banerjee, A. Kundu, P. Dey, H. Saha, and S. K. Datta, "Silica nanoparticles on front glass for efficiency enhancement in superstrate-type amorphous silicon solar cells," *J. Phys. D. Appl. Phys.*, vol. 46, no. 41, 2013.